行政院國家科學委員會專題研究計畫　成果報告

子計畫三:MPEG 多媒體傳輸機制及通訊協定在嵌入式行動平台上的分析設計(II)

計畫類別： 整合型計畫
計畫編號： NSC93-2219-E-009-019-
執行期間： 93 年 08 月 01 日至 94 年 07 月 31 日
執行單位： 國立交通大學資訊工程學系(所)

計畫主持人： 蔡淳仁

計畫參與人員： 蔡淳仁,何健鵬,張文潔,王志鵬,林君玲

報告類型： 完整報告
報告附件： 出席國際會議研究心得報告及發表論文
處理方式： 本計畫可公開查詢

中　華　民　國 94 年 10 月 31 日

行政院國家科學委員會專題研究計畫成果報告

MPEG 多媒體傳輸機制及通訊協定
在嵌入式行動平台上的分析設計

Design and Analysis of MPEG Multimedia Transport Mechanisms and Protocols for Embedded and Mobile Environment

計畫編號：NSC 93-2219-E-009-019
執行期限：93 年 8 月 1 日至 94 年 7 月 31 日

主持人：蔡淳仁　國立交通大學資訊工程系
參與人員：何健鵬、張文潔、王志鵬、林君玲　國立交通大學資訊工程系

一、中文摘要

本子計畫除了延續第一年的工作，協助 MPEG 標準制定(Test Bed for MPEG-21 Resource Delivery 已正式成為國際標準 ISO/IEC TR 21000-12），我們也根據這個 test bed 的架構，進行了兩個新的研究方向。首先是設計了一套 streaming 的流量及容錯控制機制，能夠把傳輸頻寬和封包丟失的影響考量在系統中，以到碼率最佳化（Rate-Distortion Optimized）的串流傳輸效果。

另一個研究的方向則是設計了以小波轉換(wavelet transform)為基礎之 scalable video codec 的流量控制機制。這部份的研究主要是在給定頻寬要求的前題下達到碼率失真最佳化的位元流(bitstream)切割，以供後端的串流傳輸系統進行封包包裝及傳輸的工作。而這邊所設計出來的流量控制(rate control)機制和其它系統的主要改進在於我們加入了 multiple adaptation 的考量，這對未來嵌入式行動多媒體系統（如 P2P 多媒體傳輸）的應用將有十分大的幫助。

關鍵詞：MPEG-4、MPEG-21、多媒體串流傳輸、數位內容傳輸、流量控制、嵌入式多媒體系統、碼率失真最佳化、可調式視訊壓縮。

Abstract

Our effort for this year's project follows the first year's goal to complete the standardization of our MPEG multimedia test bed. The work item has now become an International Standard (IS), ISO/IEC TR 21000-12: Test Bed for MPEG-21 Resource Delivery. For this year, we have designed two new research directions. First, we designed a streaming joint flow and error control mechanism. The proposed architecture are able to take into account both the bandwidth variation and the packet loss rate for a rate-distortion optimized (RDO) packetization and forward error correction (FEC) decision.

Another research direction is to design a multiple-adaptation capable scalable video flow control mechanism for wavelet-based scalable video codecs. This key to our research here is to achieve RD optimal bitstream adaptation for each of the multiple adaptations. The feature is crucial for future embedded multimedia applications (such as for peer-to-peer communications).

Keywords: MPEG-4, MPEG-21, multimedia streaming, digital content transport, flow control, embedded multimedia systems rate-distortion optimization, scalable video coding.

二、緣由與目的

一個完整的分散式數位多媒體系統含蓋的範圍極廣，包括數位內容的製作、數位資料庫的建立、使用者收費機制、智財權保護機制、媒體傳輸伺服器、應用服務介面，和媒體接收播放器的設計等等．為了能有一個統一的國際標準能達到建構互通的分散式多媒體系統的目的，MPEG 國際標準組織在西元2001年開始製訂一個新的國際標準：MPEG-21。

由於整個系統的重點在於能橫跨不同的網路架構和在不同的客戶端設備上（PC、手機、PDA 等等）提供一致而且最高品質的多媒體傳輸播放服務，因此傳輸系統的設計必須能動態的根據不同的平台調整。簡言之，一個數位多媒體傳輸系統的架構必需包含流量控制和容錯機制。另外，依據客戶端的能力來調整媒體資料流品質的能力也是十分重要的。

為了在頻寬和封包漏失率隨時在改變的環境下給使用者最好的串流傳輸品質，許多人嘗試對傳輸的資料進行碼率失真最佳化(Rate-Distortion)分析，然後根據分析結果來傳輸視訊串流。過去所提出的碼率失真最佳化的網路傳輸的流量控制機制裏([2] [3] [4] [5])，最大的問題在於封包漏失所造成的失真(distortion）沒有辦法量化。許多現有系統的做法在封包漏失所造成的失真的估測都十分不切實際（或完全忽略了）。我們在本年度的研究中提出了一個十分有創見的方法，可以合理的把封包失真量化。

要達到碼率失真最佳化的網路串流傳輸，除了要根據網路頻寬和封包漏失率來估測出最好的串流資料量，還必須能在算出的串流資料量限制下，從 scalable video 的位元流中，抽出最好的子位元流。所以我們針對這方面的需求，設計出了一個快速收斂的小波轉換視訊壓縮法(wavelet video coding)的流量控制機制，另外，更進一步設計了可以有效進行多次碼率最佳化的子位元流抽取的機制。

我們所設計出的碼率最佳化串流傳輸機制，也在總計畫為 MPEG 所設計出的多媒體傳輸共通測試平台上實作測試。目前此平台已經成為 MPEG 國際標準[1] 。在這個整合計畫下，總計畫團隊為 MPEG 所設計的開放原始碼包含了完整的可調式媒體伺服器、網路摸擬器、及媒體播放器。詳細的架構請參考[1]。

三、結果與討論

本計畫主要的重點在於設計 以 MPEG 技術為主的多媒體串流傳輸統。在流量控制和容錯機制的設計方面，我們進行了碼率失真最佳化（ rate-distortion optimized）可調式串流傳輸機制的設計。目前在這方面較知名的是由 P. A. Chou 等人發展的系統[2]。不過這套方法目前發表的成果以理論分析為主，在實作上有很多細節並沒有提出解決方案，而且在頻寬變化大的網路環境下，串流傳輸最難達到的平滑播放要求也沒有考量。而且這個系統有兩大缺點。首先是 Chou 使用封包漏失率來代表碼率失真最佳化分析中的失真。這是很不實際的做法。其次，他用來降低失真的方法則是預先重傳封包（非 ARQ），這也是很沒有效率的。

在可調式位元串流傳輸中，影像資料可以分成好幾次傳送，每次的傳送都可以幫助解碼端得到更接近於原影像資料的重建訊號，因此可調式位元串流的調適(scalable bitstream adaptation) 設計必須考慮到如下幾點：必須支援多樣化的更新運作(update operations)以產生有效可解碼的串流、將資料刪除時不能違反解碼相關性(decoding dependencies)的原則、允許在各個次元(dimensions)的可調性、對於媒體的特性 (如：碼率、失真率、frame rate、frame size…等)必須提供所有可能的可調適性、針對不同的調適單元(adaptation units)可能必須設計不同的調適決策、對於網路服務品質(quality of service , QoS) 設計所有可能的調適方法。媒體資源的傳遞和調適在可調適的地點 (location of adaptation) 我們可以分成：傳送端驅動調適(sender-driven adaptation)、接收端驅動調適(receiver-driven adaptation)、網路驅動調適(network-driven adaptation)等三個不同的類別來考量。

在本計畫的碼率失真最佳化串流傳輸系統中，我們把封包漏失所造成的失真，轉化為不同程度的 FEC 保護所造成的失真。舉例而言， 10^{-3} 的封包漏失率造成的失真，就相當於 10^{-3} 的 FEC 的 error protection 導致 data rate 降低所造成的失真。整個系統可以分成兩大部份：

1. 媒體封包相依性控制：媒體封包相依控制 (packet dependency control) 的設計目標是針對提供較高的錯誤抵抗能力 (higher error-resilience) 和消除影像封包的重傳 (retransmission) 需求。典型的多媒體串流在影像封包之間具有強烈的相依關係，如果其中一個影像封包在傳送過程中丟失，則與這個封包有相依關係且跟隨在後的 frames 在解碼時將可能會受到影響。網路調適性的媒體封包相依控制模組可以用來改善可調式多媒體串流的錯誤抵抗能力和減少延遲 (latency)，在此，可以運用一個樹狀的模型來記錄通道的封包丟失率 (channel loss rate) 和錯誤傳遞 (error propagation)以達成有效的控制機制。
2. 碼率失真最佳化傳輸控制：一個多媒體封包傳送的率碼失真最佳化控制架構必需在資料單元群組之間利用碼率及失真的 Lagrangian cost function 來算出最小值的解來有效率的分配時間和頻寬的網路資源。在率碼失真最佳化控制的多媒體串流系統中，決定每一個封包的 interleaving FEC 的保護程度。而這個程度則是依據此一封包的截止期限、傳送過程的歷史記錄、通道的統計資料、回饋的資訊、封包間的相依性、以及這段資料本身的 source coding 的碼率失真分析來一起進行評估。

關於這個碼率失真最佳化傳輸系統的詳細描述請參照附錄。

在快速收斂的小波轉換視訊壓縮法的流量控制機制方面，有別於一般系統慣用的查表法，我們採用的技巧是設計了一個更有效的雙參數視訊資料 R-D model 來進更最佳的子位元流切割點的快速搜尋。也因為我們所提出的視訊視訊資料 R-D model 更精簡也更有效率，我們可以把它隨著抽取出的位元流一起傳輸到接收端以進行再一次的碼率失真最佳化子位元流切割。

四、計劃成果自評

本計畫研究內容與原計畫相當符合。在達成預期目標情況方面有以下數點：

1. 完成碼率失真最佳化串流傳輸系統的開發，並將其整合到總計畫團隊為 MPEG 開發的所設計出的多媒體傳輸共通測試平台上。
2. 完成小波轉換視訊壓縮法的可進行多次碼率失真最佳化切割的流量控制機制設計。這部份的設計特別適合異質性點對點(p2p)，如從桌上電腦傳到 PDA 再傳到手機的串流傳輸。

另外，本年度計畫有待完成的部份有以下數點：

1. 未能把小波轉換視訊壓縮法移植到 MPEG 多媒體傳輸共通測試平台上。
2. 設計出來的小波轉換視訊流量控制機制未能整合到上述平台。並提供異質性點對點串流傳輸的應用示範。

以上事項預期會在第三年進行。

本年度本計畫共有一個博士生，三個碩士生參與。

附錄：A Rate-Distortion Optimized Video Streaming System with Adaptive Interleaved Forward Error Correction

1. Introduction

Multimedia streaming over IP networks is a very important trend for future communication and entertainment systems [3] . Existing IP networks adopt a best-effort approach for data delivery. As a result, bandwidth variation and/or packet losses are two common issues a multimedia streaming system must deal with in order to maintain smooth presentation with quality as constant as possible.

In order to allow smooth streaming of video data over variable bandwidth networks, scalable video coding techniques such as FGS or wavelet-based schemes are often

used [4] , [5] . With scalable video contents, a variable bitrate (VBR) source bitstream can be composed on the fly to match the channel bandwidth (assuming the bandwidth can be predicted via some model) and smoothly transmitted to the receivers for presentation. However, the video quality of the composed stream usually varies too much that it becomes visually unpleasant.

Another source of visual degradation comes from packet losses [6] , [7] . Unlike distortion from source coding, distortion due to channel loss is more difficult to quantify since the value of a single missing packet depends on the coded data it contains. Nevertheless, in order to design an R-D optimized streaming system that produces smooth and near-constant quality streams, one must find a way to formulate the distortion and rate impact of packet losses.

For scalable streaming systems, a bitstream are usually divided into base layer and enhancement layer. Base layer bitstreams contains essential information and should be protected as much as possible. In addition, the level of protection (on the texture bits) should be based on the importance of the data. To facilitate the design of the proposed R-D optimized packetization algorithm, a constant-quality rate control for the base-layer [8] , [9] is used. The encoded base layer bitstream is then protected by an adaptive FEC scheme with data-interleaving and Reed-Solomon coding.

An R-D optimized streaming framework was proposed by Chou and Miao [2] . In this scheme, the system is based on the importance and error probabilities of data units to compute transmission policies. The policy indicates whether the video packet should be transmitted at each transmission opportunity. However, the scheme does not address the issue of reducing video quality variation over loss channels. Furthermore, the mechanism maps (probability of) packet losses into rate increment of redundant packet transmission. This approach makes the resulting R-D curve impractical.

In this paper, a framework of R-D optimized video streaming is proposed. The main features of the proposed system are highlighted as follows:

- The streaming algorithm searches along the R-D curve for an optimal operating point between the scalable source coding rate and the base-layer FEC protection level. The impact of packet losses is absorbed by the level of FEC protection.
- Both video playback smoothness and visual quality consistency constraints are elegantly incorporated into the R-D optimization framework.

The rest of this paper is organized as follows. Section II presents the constant quality rate control algorithm used for the base-layer bitstream. The detail of the FEC technique used in the proposed system is described in section III. The proposed R-D optimized streaming algorithm is presented in section IV. Some experimental results and compares the proposed system with an FGS streaming system is shown in Section V. Finally, some conclusions and discussions are given in Section VI.

2. Constatnt Quality Rate Control Scheme for the Base Layer

Video bitstreams are typically encoded at a predetermined bitrate for a particular application. When the network bandwidth fluctuates, the coded bitrate may not match the real bandwidth [10] . Hence, scalable video coding techniques are often used to provide real-time quality adaptation for a streaming system. In our proposed system, data-interleaving and FEC are used to cancel the uncertainty of packet losses for R-D curve formulation. To simplify the R-D curve calculation, each texture bit should be of equal importance. Therefore, a constant quality video coding mechanism [9] is adopted in our framework for base layer encoding.

The constant-quality base layer coding scheme proposed in [9] is described as

follows. In this scheme, an initial quantization parameter is selected for the first intra encoded frame. Then, the quality of the first intra encoded frame is used for the constant-quality rate control mechanism for all base-layer frames. In practice, the quality is measured by either peak signal-to-noise ratio (PSNR) or mean square error (MSE). Under the target PSNR constraint, a constant-quality iterative coding algorithm is designed to select proper quantization parameters to minimize the video quality variation. The scheme is composed of two stages:

- **Initialization stage:**

  For the first intra encoded frame I-VOP of the base layer, the approach is to encode the frame using a given initial quantization parameter Q_0. The peak signal-to-noise ratio (PSNR) value of this frame is calculated using the luma channel of the YUV signal. I is the image of the source sequence and I' is the corresponding image at the encoder output, with pixel indices $1 \le x \le M$ and $1 \le y \le N$. The $PSNR$ is given by

$$PSNR = 10\log_{10}\left[\frac{255^2}{\frac{1}{MN}\sum_{x=1}^{M}\sum_{y=1}^{N}\left(I(x,y)-I'(x,y)\right)^2}\right]. \quad (1)$$

  Based on this formulation, the initial video quality of the first frame can be calculated and denoted by PQ_0. The PQ_0 is regarded as the constant-quality rate-control factor for the succeeding frames of the video sequence.

- **Iterative coding stage:**

1. Specify a convergence condition to control quality variation within a given range.
2. Set the starting quantization parameter value of the second frame QP_0^2 using the first initial encoded frame Q_0, and the target constant-quality factor using the PSNR of the first frame PQ_0.
3. Encode the frame k with QP_i^k.
4. Calculate the ith iteration $PSNR_i^k$, and the PSNR difference $\Delta PSNR$ is equal to PQ_0 minus $PSNR_i^k$.
5. Check $(\Delta PSNR > 0)$ $QP_i^k = QP_i^k$ -1. Otherwise $QP_i^k = QP_i^k$ +1.
6. If QP_i^k has been calculated previously, then select the minimal $\Delta PSNR$ between QP_{i-1}^k and QP_{i-2}^k, go to Step 8.
7. When the convergence condition is satisfied, then, go to Step 8. Otherwise, set the iteration index $i=i+1$ and go back to Step 2.
8. Update the reference frame using the reconstructed VOP^k for the next motion compensation operations.
9. Set the frame index $k=k+1$, the iteration index $i=0$, and $QP_0^k = QP_i^{k-1}$, go back to Step 2.

3. Error Control and Packetization for base layer

The base-layer bitstream of a scalable sequence contains the most essential video content. When the base-layer bitstream cannot be recovered from transmission errors, the corresponding enhancement layer is useless even if they arrive at the client side successfully [11] , [12] . Consequently, the base-layer should be strongly protected against packet loss or corruption [13] . Furthermore, a base layer bitstream free from packet losses (through FEC protection) makes R-D calculation deterministic and therefore an R-D optimal streaming system can be practically constructed.

Forward error correction (FEC) is an important low-delay mechanism for reducing or eliminating packet losses [14] in a streaming system. This section presents the FEC technique used in the proposed framework. The FEC combines data-interleaving and Reed-Solomon (RS) coding.

For base-layer data, a (*n*, *k*) Reed-Solomon code-based FEC is applied to add resiliency to the original bitstream. In Fig. 1 (a), *n* is the codeword length of the Reed-Solomon encoder, *k* is the number of base-layer bitstream symbols, and s is the number of correctable symbols. The number of parity symbols is 2*s*, where 2*s* = *n* – *k*. If burst-errors occur during transmission, then the Reed-Solomon decoder can correct up to s errors and detect up to 2*s* errors per codeword. When packet loss is detected in the client application, the Reed-Solomon decoder may have sufficient information to allow successful reconstruction of the original video.

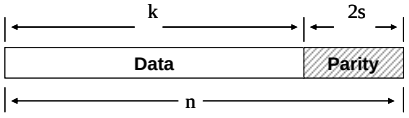

(a)

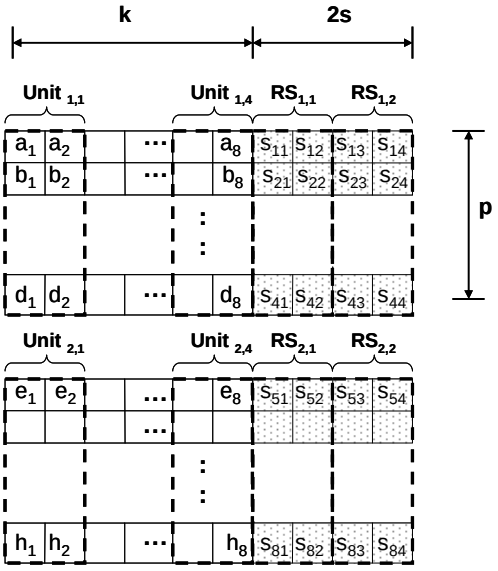

(b)

Fig. 1. (a) A (*n*, *k*) Reed Solomon code, and (b) One GOP on the base layer in the pre-interleaving stage. In this example, *n*=12, *k* =8, *s* =2, *p*=4, and *q*=2.

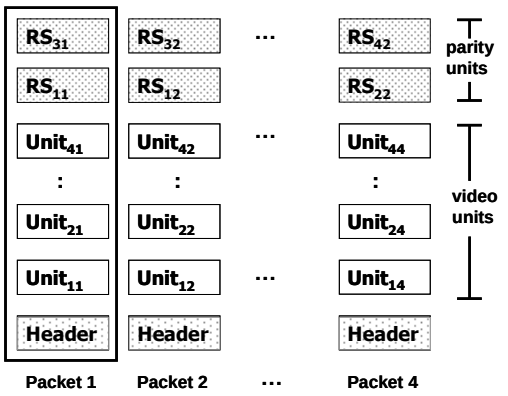

Fig. 2. Packetization scheme for one GOP on the base layer. In this example, *n*=12, *k* =8, *s* =2, *p*=4, and *q*=2.

In [16] , two FEC packetization schemes for single-layer video were proposed. However, they do not perform data-interleaving. To reduce packet header overhead while maintain packet loss resiliency, a data-interleaving scheme is used to shuffle the RS coded data among several data packets before transmission. Generally, a high error rates channel can be defined as medium losses (2%–5% packet loss) or heavy losses (5% packet loss) [15] . When base-layer bitstream is transmitted over the high error rates channel, a codeword may contain more than *s* symbol errors due to packet losses or bit errors. Moreover, the decoding process may fail to recover the bitstream symbols. As shown in Fig. 1 (b), a group of picture (GOP) is split into several groups of equal length, where the length of a group is *p* symbols. Each interleaved group is composed of *q* symbols from each codeword. Fig. 2 shows the proposed interleave scheme under a (*n*, *k*) Reed-Solomon code. In this case, the Reed-Solomon decoder is able to recover from *s* / *q* = 1 loss packets in one group, where the total number of packets for one GOP is (*n*-2*s)* / *q* = 4.

4. Proposed streaming framework

A piecewise-linear model and a piecewise- exponential model can be used for modeling the rate-distortion (R-D) curve of enhancement-layer bitstream [8] , [10] . And the quality variation can be reduced by using

the models in finding an optimal constant quality constrained rate allocation from two neighboring sampling points. But to produce an optimal R-D solution, the increase of computation time is a drawback for real-time applications.

To reduce the computational cost of the rate allocation, each bit plane is treating as a transmission unit in the enhancement layer. In addition, experiments show that the video quality near step-wise increases as the number of decoded bit-planes increases. Hence, a left/right comparison scheme is used to find the number of bit-plane preserved in the enhancement-layer bitstream for minimizing the variation in video quality. The left/right comparison scheme select a minimum quality variation among neighboring bit-planes {BP-1, BP} or {BP, BP+1}. The rate allocation aims to allocate bits for smoothing the average video quality at discrete transmission time, subject to an available bit rate constraint. The layer truncation algorithm (ELT) is described below.

- **Description of ELT**

1. R-D costs of FGS enhancement- layer bitstreams are extracted at the end of each bit-plane. And is stored into a disk file for further analysis.
2. Given an initial protection level p, and a remaining bandwidth is computed as $\kappa(i) = BW_i - \sum_{n=i}^{n=i+w} I_n(p)$, where BWi is the available bandwidth of the ith transmitting period, In(p) is the size of the interleaved base-layer bitstream of frame n under FEC by Reed-Solomon coding, and coded using GOP size w .
3. If the value of $\kappa(i)$ is negative, then reducing the value of protection level p=p-1, go to Step 2.
4. Given a remaining bandwidth, using the amount of bits generated by each bit-plane to estimate a target PSNR ratio for the first GOP.
5. The left/right comparison scheme is applied to find the number of bit-plane preserved in enhancement layer of frame n and to smooth out the inter-frame quality variation.
6. Compute the consumed bits of each bit-plane in the GOP: $\psi(i) = \kappa(i) - \sum_{n=i}^{n=i+w} E_n(\eta)$, where $E_n(\eta)$ is the size of the preserved bit-plane of frame n
7. If the remaining bandwidth allowed, then increase the number of bit-planes, and go back to step 4.
8. Selected a GOP in a minimal quality variation based on the average PSNR values of the previous GOP.
9. Assign more protection to the base-layer bitstream when transmission conditions become worse.
10. Process the next GOP until the end of the frame.

5. Experimental Results

This section presents the experimental results of the proposed video streaming system. A block diagram of the proposed streaming system is shown in Fig. 3. The system is based on the MPEG-21 Test Bed for Resource Delivery [17] . The test bed is able to emulate media resource delivery with a network emulator (based on NIST Net [18]) that allows real-time simulation of common network conditions. We have added Reed-Solomon coding modules, an interleaver module, and a de-interleaver module to the original test bed.

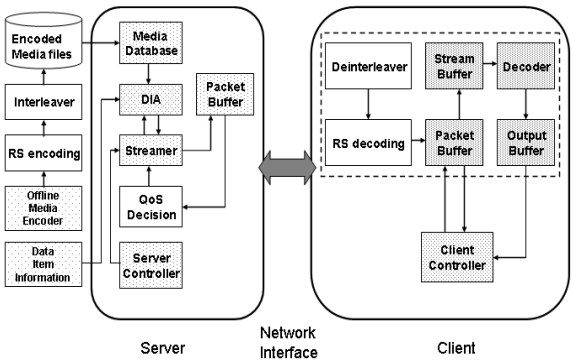

Fig. 3. Architecture of the proposed system

To validate the effectiveness of the R-D optimized video streaming system which we have described in this paper, we use the Akiyo, Coastguard, Foreman, Mobile, and Stefan sequences that are the standard test

sequences of MPEG-4 as our experimental sequences. The parameters are set as follows: The format of those sequences is CIF (352*288). Those sequences are encoded using ISO/IEC 14496 (MPEG-4) visual reference software (Microsoft-FDAM1-2.5-040207) at 10 frames per second. The coding mode is one I-frame followed by nine P-frames.

Fig. 4Fig. 5and Fig. 6shows the R-D curves between source rate, expect distortion and the one protected by different RS-level (RS(255,247,9) – RS(255,127, 129)) bitstream in the sequence. Those experimental results are based on the channel rate 400 kbps, and QP=15. Table 1, Table 2, and Table 3 show the selected frames 31th (I-frame), 32th (P-frame) and 33th (P-frame) frames for presenting the number of average bit error per codeword of the Stefan sequence respectively. Those experimental results are based on the channel rate 300 kbps.

Fig. 7shows the R-D curves between source rates and the expect distortion by adding different enhancement-layer bitstream in the sequence. Fig. 8shows R-D slope between source rates and slope variation in the Mobile sequence. As the figure shows, a slope rating increases slowly at the beginning part of the bit-plane. On the contrary, a slope rating may increase sharply from the middle part to the end part of the bit-plane. Fig. 9and Fig. 10show the system try to include the points on the convex hull. From Fig. 11to Fig. 18 show the experimental results on the 32th and 33th frames in the mobile sequence. From Fig. 19to Fig. 28show the experimental results from the 31th and 33th frames in the stefan sequence.

To investigate the system performance under different traffic loads and different video, Fig. 29 shows the channel condition used in our simulation environment. The first bandwidth plan begins at 50 kbps, increases to 100 kbps at the third second, continuous drops to 38 kbps until 7th second, recovers back to 110 kbps at 8th second, and then increases to 119 kbps. From the second to the fifth bandwidth plan are shown in Fig. 32, Fig. 35, Fig. 38 and Fig. 41. In addition, Fig. 30, Fig. 33, Fig. 36, Fig. 39 and Fig. 42show PSNR values for the Akiyo, Coastguard, Foreman, Mobile, and Stefan sequences respectively. The streaming algorithm searches along the R-D curve for an optimal operating point between the scalable source coding rate and the base-layer FEC protection level. When the transmission rate fluctuates significantly, e.g., from the 50th to the 70th frame, the proposed system can increase the base-layer FEC protection level, adapt the bandwidth changing quickly and reduce the degree of quality variation. Fig. 31, Fig. 34, Fig. 37, Fig. 40 and Fig. 43show the bit rate variation of the FEC protected base-layer and applying enhancement-layer bitstream under the variable bandwidth condition. For example, when the transmission rate changes from 528kbps to 418kbps, the higher levels of channel protection is applied to the base-layer of Mobile sequence than increases more enhancement-layer(s) bitstream to enhance the base layer, so that most of the enhancement-layer bitstream is truncated during the period.

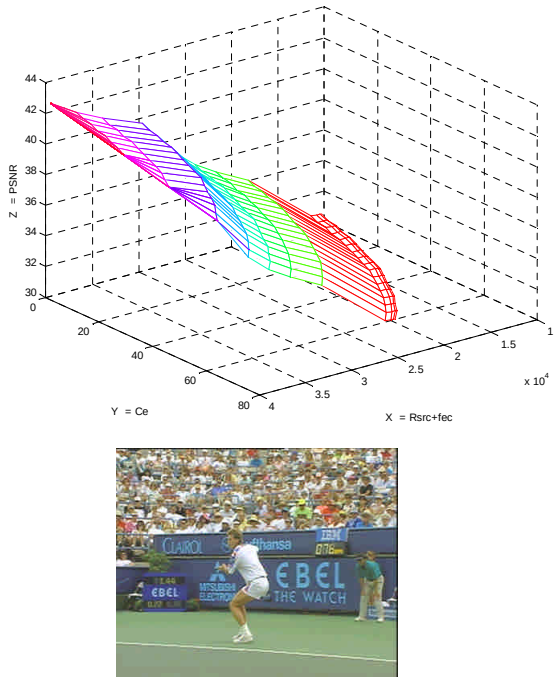

Fig. 4. R-D curves between source rate, expect distortion and the one protected by different RS-level (RS(255,247,9) – RS(255,127, 129)) bitstream in the *Stefan* sequence. (31th frame, I-frame)

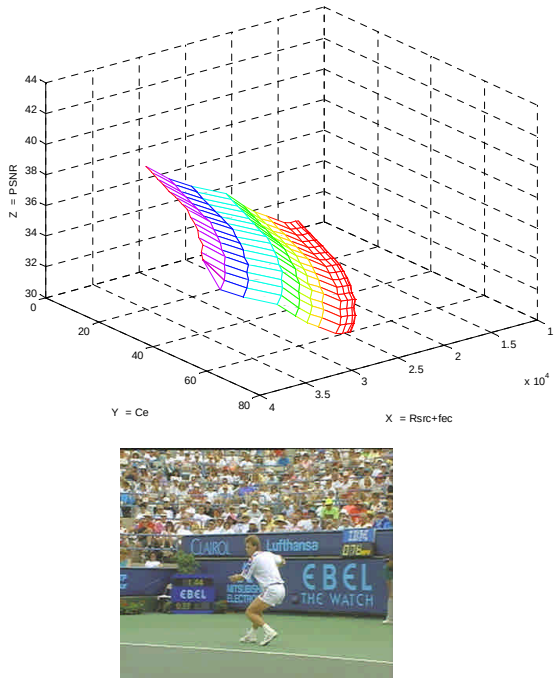

Fig. 5. R-D curves between source rate, expect distortion and the one protected by different RS-level (RS(255,247,9) – RS(255,127, 129)) bitstream in the *Stefan* sequence. (32th frame, P-frame)

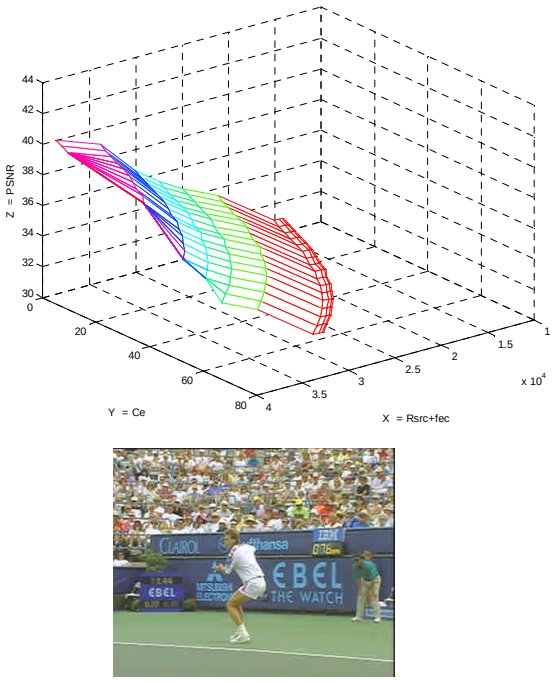

Fig. 6. R-D curves between source rate, expect distortion and the one protected by different RS-level (RS(255,247,9) – RS(255,127, 129)) bitstream in the *Stefan* sequence. (33th frame, P-frame)

Table 1. The number of average bit error per codeword for 31th frame (I-frame) on the base layer (Stefan sequence)

RS code	RS248	RS240	RS232	RS224	RS216	RS208	RS200	RS192	RS184	RS176	RS168	RS160	RS152	RS144	RS136	RS128
# of correctable symbols	4	8	12	16	20	24	28	32	36	40	44	48	52	56	60	64
$5*10^{-2}$	35.71429	34.88372	33.33333	32.6087	31.25	30	28.84615	27.77778	26.78571	25.42373	24.19355	23.07692	22.05882	20.83333	19.73684	18.51852
$2.5*10^{-2}$	17.85714	17.44186	16.66667	16.30435	15.625	15	14.42308	13.88889	13.39286	12.71186	12.09677	11.53846	11.02941	10.41667	9.868421	9.259259
10^{-2}	7.142857	6.976744	6.666667	6.521739	6.25	6	5.769231	5.555556	5.357143	5.084746	4.83871	4.615385	4.411765	4.166667	3.947368	3.703704
$5*10^{-3}$	3.571429	3.488372	3.333333	3.26087	3.125	3	2.884615	2.777778	2.678571	2.542373	2.419355	2.307692	2.205882	2.083333	1.973684	1.851852
10^{-4}	0.714286	0.697674	0.666667	0.652174	0.625	0.6	0.576923	0.555556	0.535714	0.508475	0.483871	0.461538	0.441176	0.416667	0.394737	0.37037
$5*10^{-4}$	0.357143	0.348837	0.333333	0.326087	0.3125	0.3	0.288462	0.277778	0.267857	0.254237	0.241935	0.230769	0.220588	0.208333	0.197368	0.185185

Table 2. The number of average bit error per codeword for 32th frame (P-frame) on the base layer (Stefan sequence)

RS code	RS248	RS240	RS232	RS224	RS216	RS208	RS200	RS192	RS184	RS176	RS168	RS160	RS152	RS144	RS136	RS128
# of correctable symbols	4	8	12	16	20	24	28	32	36	40	44	48	52	56	60	64
$5*10^{-2}$	28.84615	27.77778	26.78571	25.86207	25	24.19355	23.4375	22.38806	21.42857	20.54795	19.48052	18.75	17.64706	16.85393	15.95745	15
$2.5*10^{-2}$	14.42308	13.88889	13.39286	12.93103	12.5	12.09677	11.71875	11.19403	10.71429	10.27397	9.74026	9.375	8.823529	8.426966	7.978723	7.5
10^{-2}	5.769231	5.555556	5.357143	5.172414	5	4.83871	4.6875	4.477612	4.285714	4.109589	3.896104	3.75	3.529412	3.370787	3.191489	3
$5*10^{-3}$	2.884615	2.777778	2.678571	2.586207	2.5	2.419355	2.34375	2.238806	2.142857	2.054795	1.948052	1.875	1.764706	1.685393	1.595745	1.5
10^{-4}	0.576923	0.555556	0.535714	0.517241	0.5	0.483871	0.46875	0.447761	0.428571	0.410959	0.38961	0.375	0.352941	0.337079	0.319149	0.3
$5*10^{-4}$	0.288462	0.277778	0.267857	0.258621	0.25	0.241935	0.234375	0.223881	0.214286	0.205479	0.194805	0.1875	0.176471	0.168539	0.159574	0.15

Table 3. The number of average bit error per codeword for 33th frame (P-frame) on the base layer (Stefan sequence)

RS code	RS248	RS240	RS232	RS224	RS216	RS208	RS200	RS192	RS184	RS176	RS168	RS160	RS152	RS144	RS136	RS128
# of correctable symbols	4	8	12	16	20	24	28	32	36	40	44	48	52	56	60	64
$5*10^{-2}$	26.31579	25.42373	24.59016	23.80952	23.07692	22.05882	21.12676	20.54795	19.48052	18.75	17.85714	17.04545	16.12903	15.30612	14.42308	13.63636
$2.5*10^{-2}$	13.15789	12.71186	12.29508	11.90476	11.53846	11.02941	10.56338	10.27397	9.74026	9.375	8.928571	8.522727	8.064516	7.653061	7.211538	6.818182
10^{-2}	5.263158	5.084746	4.918033	4.761905	4.615385	4.411765	4.225352	4.109589	3.896104	3.75	3.571429	3.409091	3.225806	3.061224	2.884615	2.727273
$5*10^{-3}$	2.631579	2.542373	2.459016	2.380952	2.307692	2.205882	2.112676	2.054795	1.948052	1.875	1.785714	1.704545	1.612903	1.530612	1.442308	1.363636
10^{-4}	0.526316	0.508475	0.491803	0.47619	0.461538	0.441176	0.422535	0.410959	0.38961	0.375	0.357143	0.340909	0.322581	0.306122	0.288462	0.272727
$5*10^{-4}$	0.263158	0.254237	0.245902	0.238095	0.230769	0.220588	0.211268	0.205479	0.194805	0.1875	0.178571	0.170455	0.16129	0.153061	0.144231	0.136364

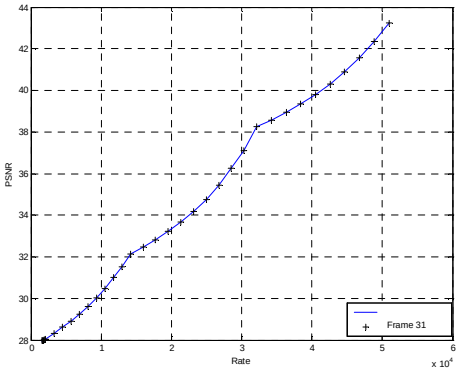

Fig. 7. R-D curves between source rates and expect distortion in the Mobile sequence. (31th frame, I-frame)

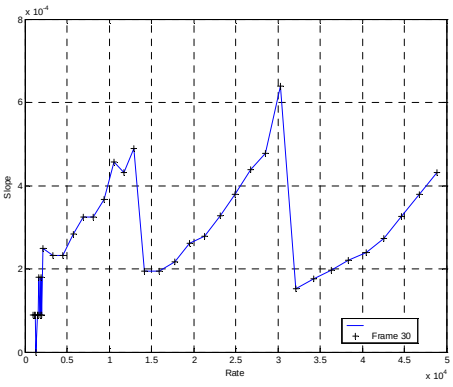

Fig. 8. R-D slope between source rates and slope variation in the Mobile sequence. (31th frame, I-frame)

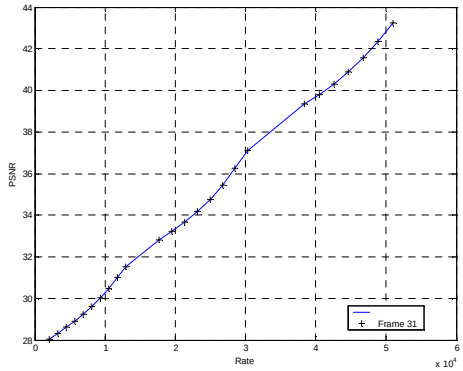

Fig. 9. R-D curves between source rates and expect distortion in the Mobile sequence. (s>0.0002 , 31th frame, I-frame)

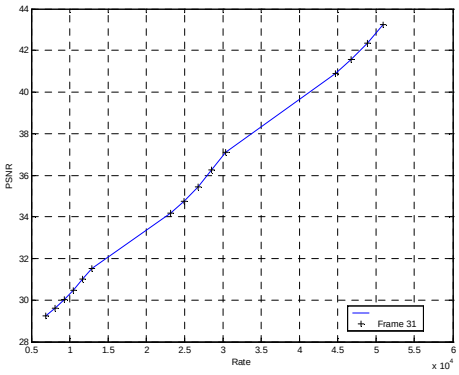

Fig. 10. R-D curves between source rates and expect distortion in the Mobile sequence. (s>0.0003 , 31th frame, I-frame)

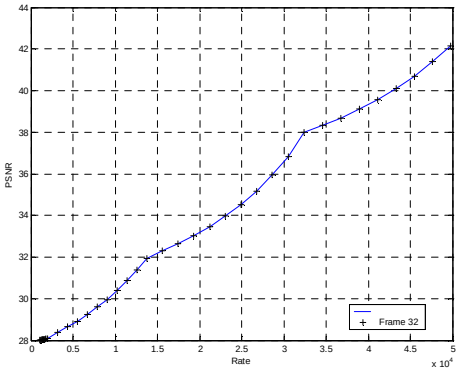

Fig. 11. R-D curves between source rates and expect distortion in the Mobile sequence. (32th frame, P-frame)

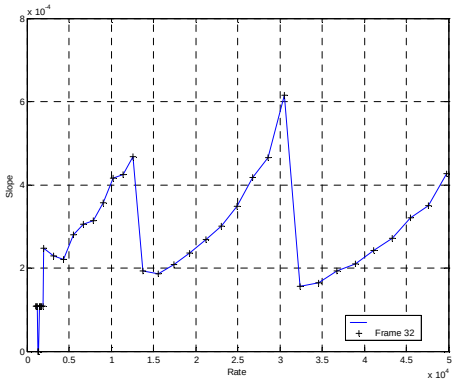

Fig. 12. R-D slope between source rates and slope variation in the Mobile sequence. (32th frame, P-frame)

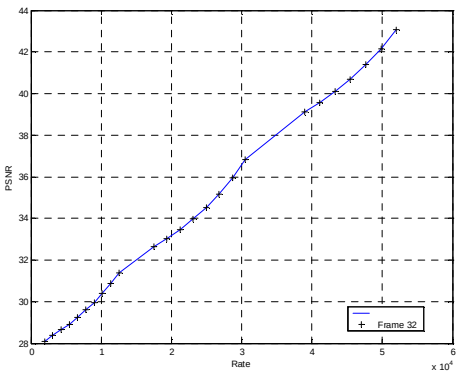

Fig. 13. R-D curves between source rates and expect distortion in the Mobile sequence. (s>0.0002 , 32th frame, P-frame)

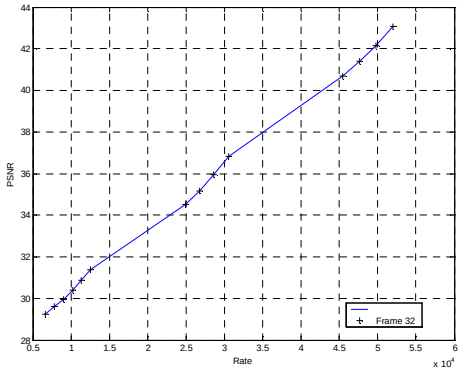

Fig. 14. R-D curves between source rates and expect distortion in the Mobile sequence. (s>0.0003 , 32th frame, P-frame)

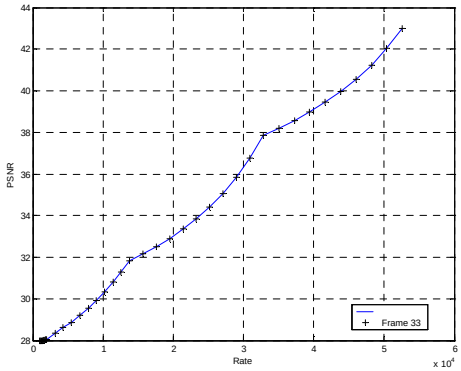

Fig. 15. R-D curves between source rates and expect distortion in the Mobile sequence. (33th frame, P-frame)

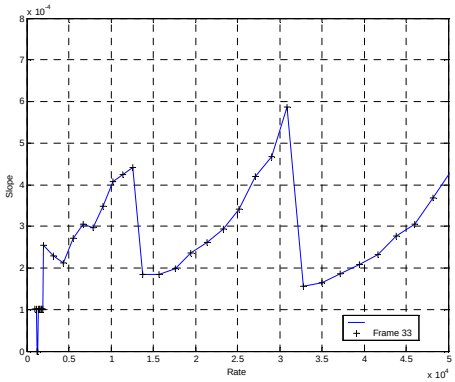

Fig. 16. R-D slope between source rates and slope variation in the Mobile sequence. (33th frame, P-frame)

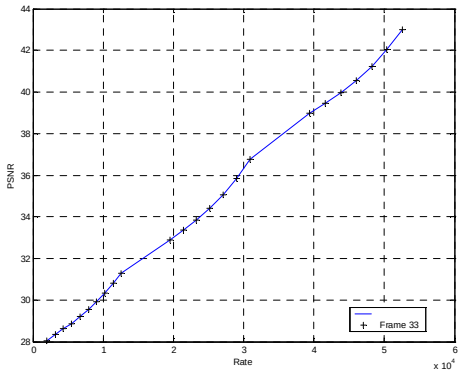

Fig. 17. R-D curves between source rates and expect distortion in the Mobile sequence. (s>0.0002 , 33th frame, P-frame)

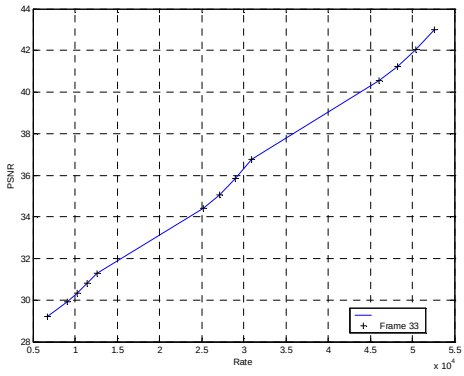

Fig. 18. R-D curves between source rates and expect distortion in the Mobile sequence. (s>0.0003 , 33th frame, P-frame)

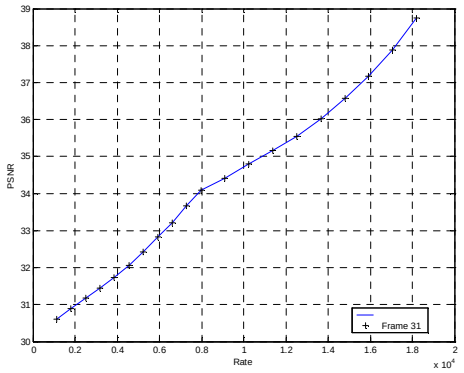

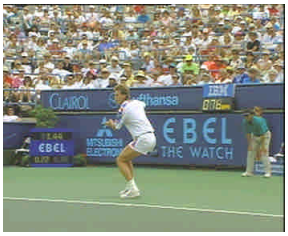

Fig. 19. R-D curves between source rates and expect distortion in the *Stefan* sequence. (31th frame, I-frame)

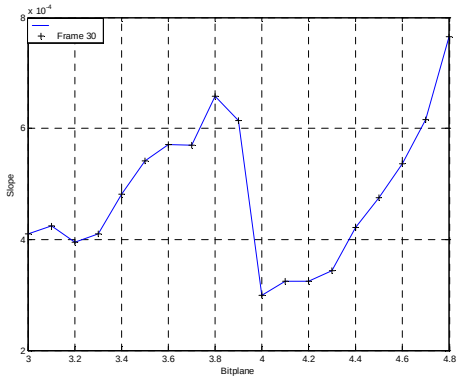

Fig. 20. R-D slope between bit-planes and slope variation in the *Stefan* sequence. (31th frame, I-frame)

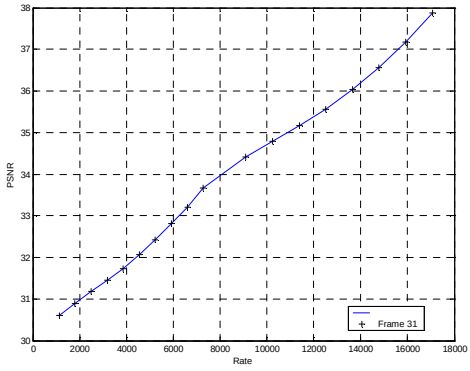

Fig. 21. R-D curves between source rates and expect distortion in the *Stefan* sequence. (s>0.0003 , 31th frame, I-frame)

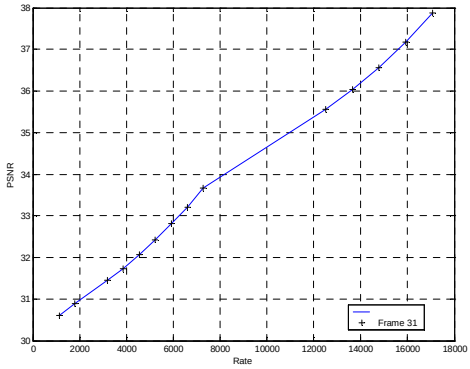

Fig. 22. R-D curves between source rates and expect distortion in the *Stefan* sequence. (s>0.0004 , 31th frame, I-frame)

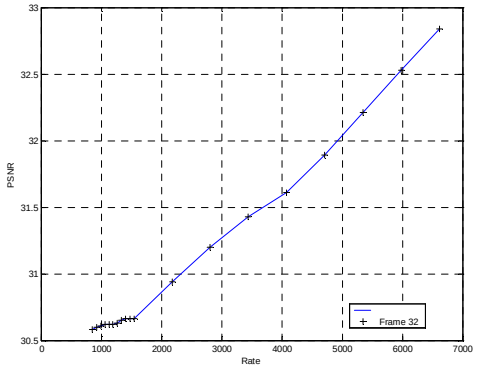

Fig. 23. R-D curves between source rates and expect distortion in the *Stefan* sequence. (32th frame, P-frame)

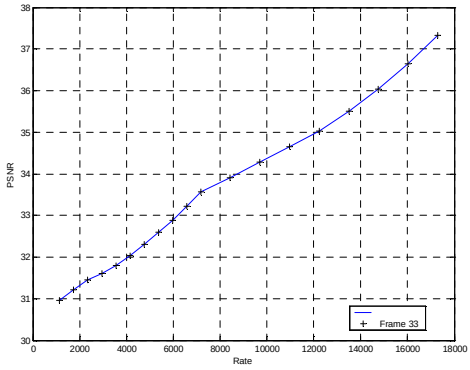

Fig. 26. R-D curves between source rates and expect distortion in the *Stefan* sequence. (33th frame, P-frame)

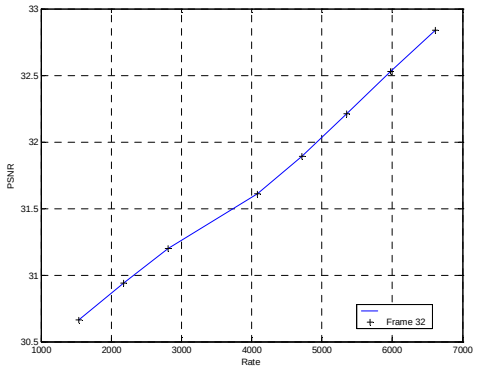

Fig. 24. R-D curves between source rates and expect distortion in the *Stefan* sequence. (s>0.0003 , 32th frame, P-frame)

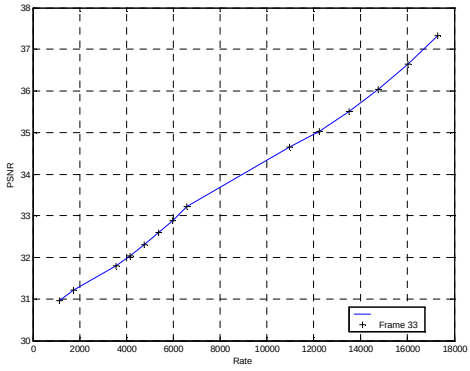

Fig. 27. R-D curves between source rates and expect distortion in the *Stefan* sequence. (s>0.0003 , 33th frame, P-frame)

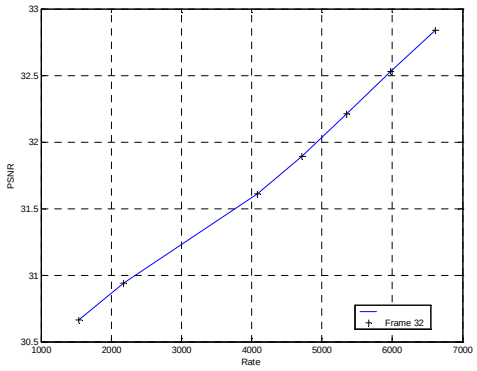

Fig. 25. R-D curves between source rates and expect distortion in the *Stefan* sequence. (s>0.0004 , 32th frame, P-frame)

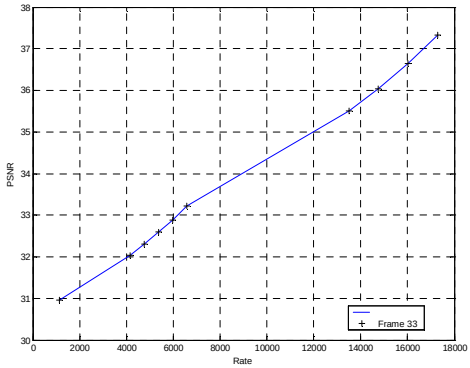

Fig. 28. R-D curves between source rates and expect distortion in the *Stefan* sequence. (s>0.0004 , 33th frame, P-frame)

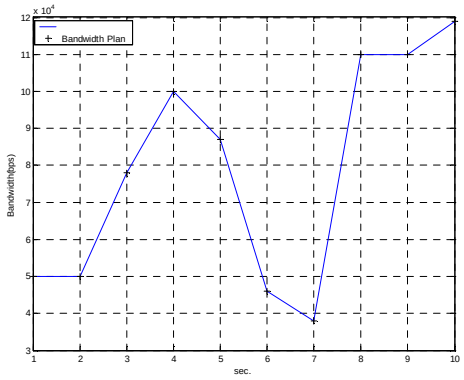

Fig. 29. Dynamic channel condition illustrating available bandwidth for *Akiyo* sequence.

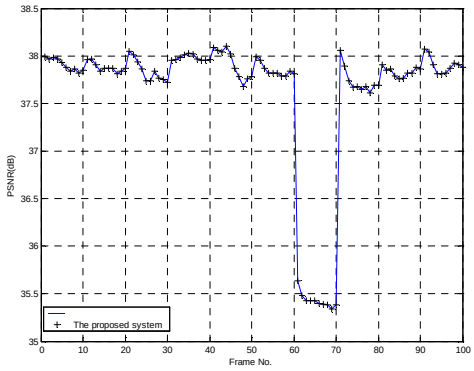

Fig. 30. PSNR performance for *Akiyo* sequence.

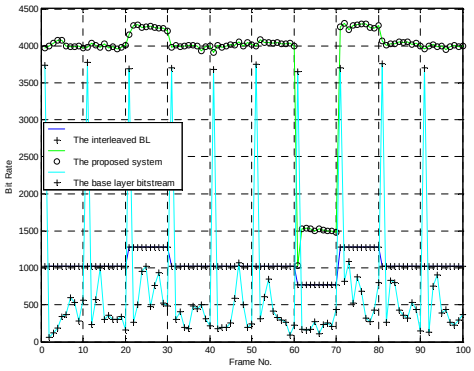

Fig. 31. Bitrates for the base layer bitstream, the FEC-protected base-layer and enhance the perceived quality by applying more enhancement-layer bitstream for *Akiyo* sequence.

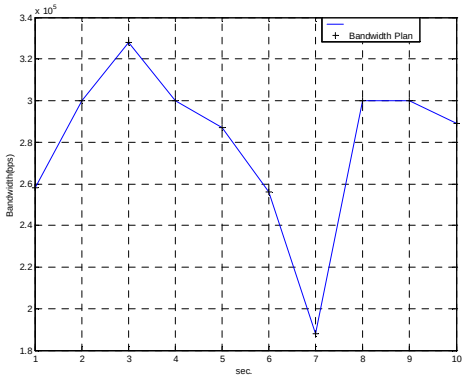

Fig. 32. Dynamic channel condition illustrating available bandwidth for *Coastguard* sequence.

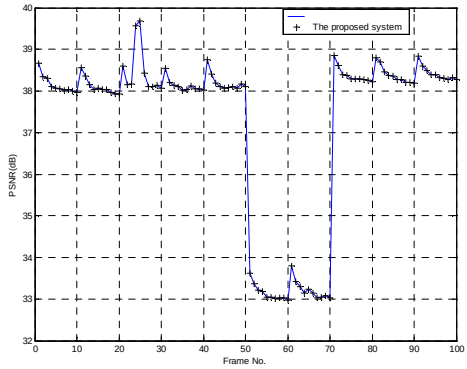

Fig. 33. PSNR performance for *Coastguard* sequence.

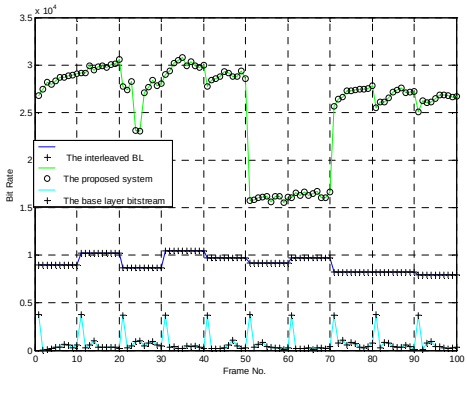

Fig. 34. Bitrates for the base layer bitstream, the FEC-protected base-layer and enhance the perceived quality by applying more enhancement-layer bitstream for *Coastguard* sequence.

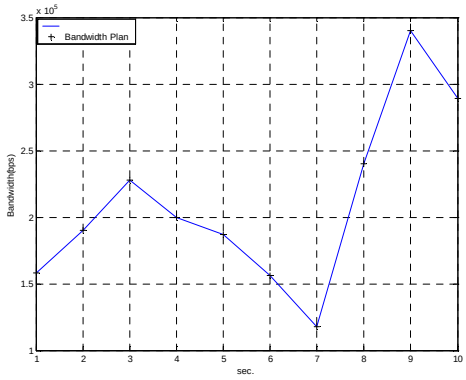

Fig. 35. Dynamic channel condition illustrating available bandwidth for *Foreman* sequence.

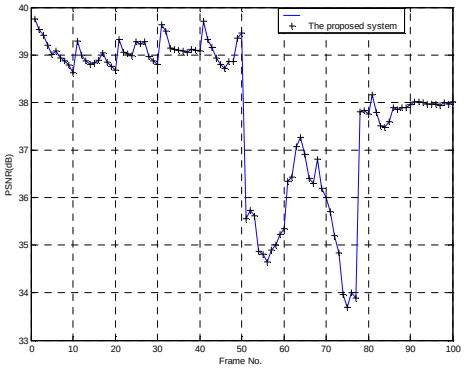

Fig. 36. PSNR performance for *Foreman* sequence.

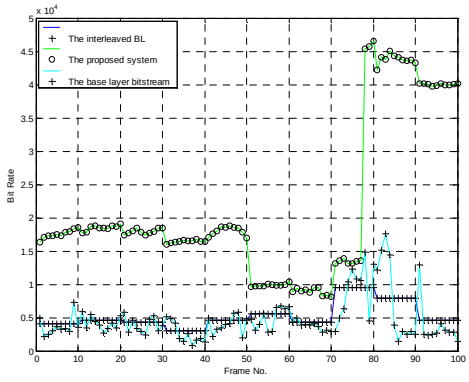

Fig. 37. Bitrates for the base layer bitstream, the FEC-protected base-layer and enhance the perceived quality by applying more enhancement-layer bitstream for *Foreman* sequence.

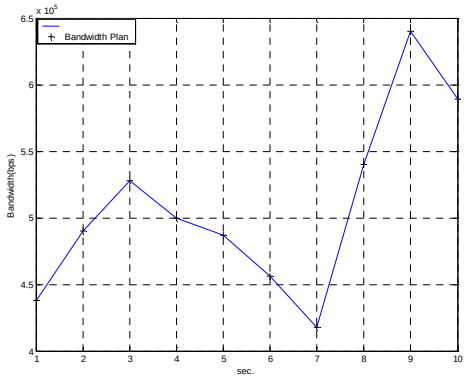

Fig. 38. Dynamic channel condition illustrating available bandwidth for *Mobile* sequence.

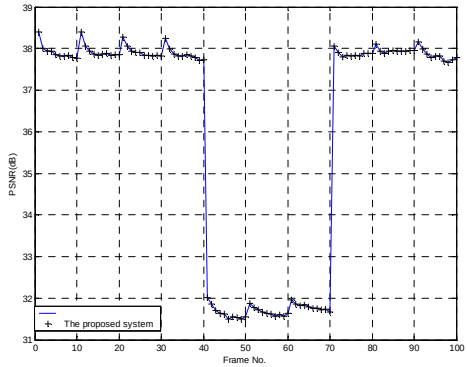

Fig. 39. PSNR performance for *Mobile* sequence.

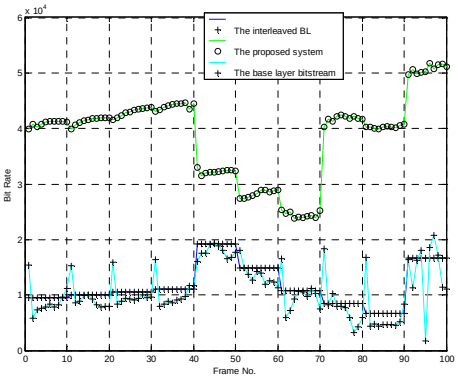

Fig. 40. Bitrates for the base layer bitstream, the FEC-protected base-layer and enhance the perceived quality by applying more enhancement-layer bitstream for *Mobile* sequence.

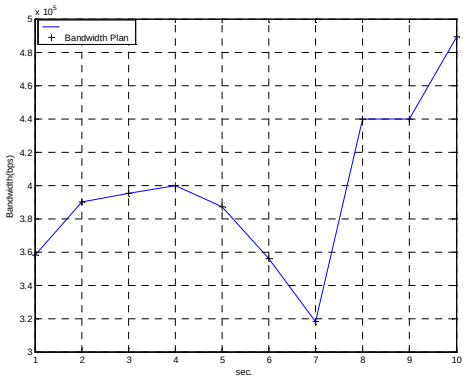

Fig. 41. Dynamic channel condition illustrating available bandwidth for *Stefan* sequence.

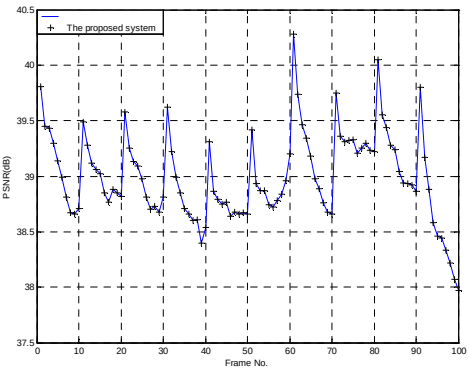

Fig. 42. PSNR performance for *Stefan* sequence.

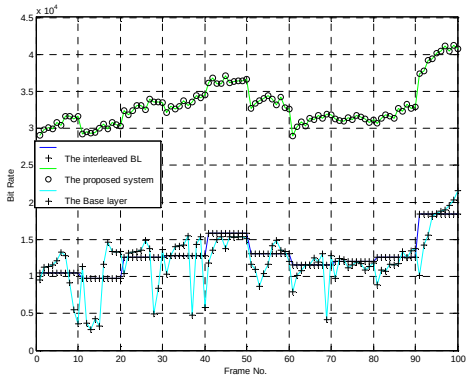

Fig. 43. Bitrates for the base layer bitstream, the FEC-protected base-layer and enhance the perceived quality by applying more enhancement-layer bitstream for *Stefan* sequence.

For a full system experiments, we used the CIF version of the FOREMAN sequence is used. The sequence is encoded using ISO/IEC 14496 (MPEG-4) visual reference software (Microsoft-FDAM1-2.5-040207) at 10 frames per second. The coding mode is one I-frame followed by nine P-frames at 10 frames per second. Fig. 44 presents the PSNR performance of the streaming system under a variable bandwidth scenario, ranging from 68kbps to 240kbps. When the transmission rate fluctuates significantly, e.g., from the 40th to the 80th frame, the proposed system can adapt the bandwidth changing quickly and reduce the degree of quality variation. Fig. 45 shows the bit rate of the encoded base-layer bitstream, and the bit rate of RS(255, 251, 5)/RS(255, 223, 33) protection level bitstream. Fig. 46 shows the bit rate variation of the FEC protected base-layer and enhancement-layer bitstream under the variable bandwidth condition. For example, when the transmission rate changes from 180kbps to 116kbps, the system performs dynamic rate allocation to add more FEC protection on the base-layer. Consequently, most of the enhancement-layer bitstream is truncated during the period.

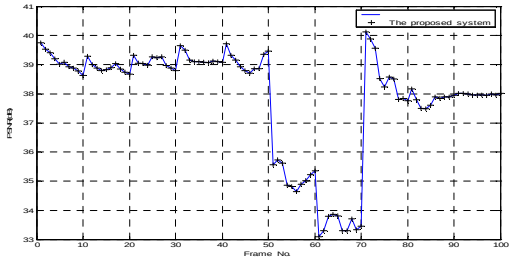

Fig. 44. PSNR under variable transmission rates.

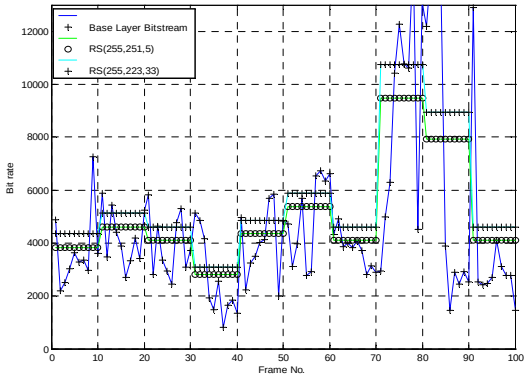

Fig. 45. Bitrates of the original and the FEC-protected base-layer bitstreams.

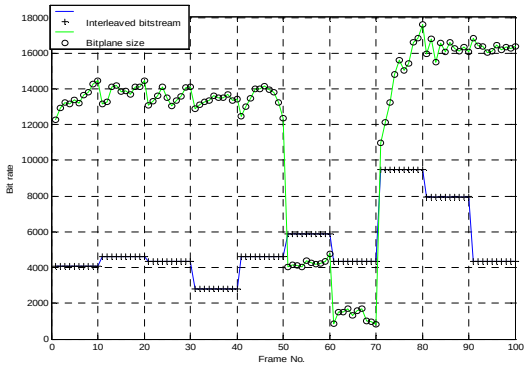

Fig. 46. Bitrates for the FEC-protected base-layer and the enhancement-layer bitstreams.

五、參考文獻

[1] ISO/IEC JTC 1/SC 29, *Inofrmation Technology – Multimedia Framework (MPEG-21) – Part 12: Test Bed for MPEG-21 Resource Delivery*, *ISO/IEC TR 21000-12: 2004(E)*, 2004.

[2] P. A. Chou and Z. Miao, "Rate-distortion optimized streaming of packetized media," IEEE Transactions on Multimedia, February 2001.

[3] M. R. Civanlar, "Internet video - Protocols & applications," in Proc. Packet Video Workshop 2001, 2001.

[4] M. Dai and D. Loguinov, "Analysis of Rate-Distortion Functions and Congestion Control in Scalable Internet Video Streaming," ACM NOSSDAV, June 2003.

[5] Chuo-Ling Chang, Sangeun Han, and Bernd Girod, "Rate-Distortion Optimized Streaming for 3-D Wavelet Video," Proc. IEEE International Conference on Image Processing, Singapore, Oct. 2004.

[6] Anirban Mahanti, Derek L. Eager, Mary K.

Vernon, David J. Sundaram-Stukel, "Scalable on-demand media streaming with packet loss recovery," IEEE/ACM Transactions on Networking, vol. 11, no. 2, pp. 195-209, Apr 2003.

[7] T. Nguyen and A. Zakhor, "Protocols for Distributed Video Streaming," in International Conference on Image Processing 2002, Rochester, New York, Vol. 3, p. 185-189, September 2002.

[8] Lefeng Zhao, JongWon Kim, and C.-C. Jay Kuo, "Constant quality rate control for streaming MPEG-4 FGS video," IEEE International Symposium on Circuits and Systems, Vol. 4, pp.544-547, May 2002.

[9] Jun Sun, Wen Gao, and Qingming Huang, "A Novel FGS Base-Layer Encoding Model and Weight-Based Rate Adaptation for Constant-Quality Streaming," Proc. Third International Conference on Image and Graphics, pp. 373 – 376, Dec 2004.

[10] Xi Min Zhang, Anthony Vetro, Yun Q.Shi, and Huifang Sun, "Constant Quality Constrained Rate Allocation for FGS Video Coded Bitstreams, " IEEE Transactions on Circuits and Systems for Video Technology, Vol. 13, No. 2, pp. 121-130, Feb 2003.

[11] J. Zhou, H. Shao, C. Shen and M.T. Sun, "Multi-path Transport of FGS Video," Packet Video Workshop, 2003.

[12] Charfi, Y., Hamzaoui, R., "Packet loss protection of scalable video bitstreams using forward error correction and feedback," International Symposium on Image and Signal Processing and Analysis, Rome, September 2003.

[13] K. W. Stuhlmueller, M. Link, B. Girod and U. Horn, "Scalable Internet Video Streaming With Unequal Error Protection", Packet Video Workshop, New York, 26/27 April 1999.

[14] Huahui Wu, Mark Claypool, Robert Kinicki, "A Model for MPEG with Forward Error Correction and TCP Friendly Bandwidth, " In Proceedings of Workshop on Network and Operating Systems Support for Digital Audio and Video (NOSSDAV), Monterey, California, USA, June 2003.

[15] Bo Yan, Kam Wing Ng, "Mode-based error-resilient techniques for the robust communication of MPEG-4 video ", IEEE Transactions on Circuits and Systems for Video Technology, Vol. 14, No.6, pp. 874-879, 2004.

[16] F. Zhai, Y. Eisenberg, C. E. Luna, T. N. Pappas, R. Berry, and A. K. Katsaggelos, "Packetization Schemes for Forward Error Correction in Internet Video Streaming," Proc. 41st Allerton Conference Communication, Control, and Computing, October 2003.

[17] MPEG-21 Test Bed for Resource Delivery, http://clabprj.ee.nctu.edu.tw/~mpeg21tb/

[18] Mark Carson and Darrin Santay, "NIST Net: a Linux-based networkemulation tool", Computer Communication Review (ACM SIGCOMM), 33(3), pp. 111-126, 2003.